

# Inhibitory Effects and Molecular Mechanisms of Selenium-Containing Tea Polysaccharides on Human Breast Cancer MCF-7 Cells

Nianwu He,<sup>†,‡</sup> Xiaolong Shi,<sup>†</sup> Yan Zhao,<sup>§</sup> Lingmin Tian,<sup>†</sup> Dongying Wang,<sup>†</sup> and Xingbin Yang<sup>\*,†</sup>

<sup>†</sup>Key Laboratory of Ministry of Education for Medicinal Resource and Natural Pharmaceutical Chemistry, College of Food Engineering and Nutritional Science, Shaanxi Normal University, Xi'an 710062, China

<sup>‡</sup>Department of Biopharmaceutical Engineering, Shangluo University, Shangluo 726000, China

<sup>§</sup>School of Pharmacy, Fourth Military Medical University, Xi'an 710032, China

**ABSTRACT:** Dietary supplementation of selenium-enriched tea is known to have an anticancer health benefit. This study was to investigate the inhibitory effect of selenium-containing tea polysaccharides (Se-GTPs) from a new variety of selenium-enriched Ziyang green tea against human MCF-7 breast cancer cells. Se-GTPs dose-dependently exhibited an effective cell growth inhibition with an IC<sub>50</sub> of 140.1 μg/mL by inducing MCF-7 cancer cells to undergo G2/M phase arrest and apoptosis. The blockade of cell cycle was associated with an up-regulation of p53 expression, but not CDK2. Se-GTPs clearly triggered the mitochondrial apoptotic pathway, as indicated by an increase in Bax/Bcl-2 ratio and subsequent caspase-3 and caspase-9 activation. It was also found that the generation of intracellular ROS is a critical mediator in Se-GTPs-induced cell growth inhibition. These findings suggest that Se-GTPs may serve as a potential novel dietary agent for human breast cancer chemoprevention.

**KEYWORDS:** tea polysaccharide, selenium, breast cancer, MCF-7 cells, apoptosis

## ■ INTRODUCTION

Selenium is a naturally occurring micronutrient with essential biological functions and belongs to the most extensively studied chemopreventive compounds.<sup>1,2</sup> Foods (cereals, grains, vegetables) contain diverse amounts and chemical forms of selenium.<sup>1</sup> An adequate selenium intake has been estimated at 50 μg/day with toxic levels being estimated to occur with intakes on the order of 350–700 μg/day.<sup>1</sup> Inorganic selenite can be transformed into organic forms via binding with proteins and polysaccharides in various organisms, which are considered as more effective and secure.<sup>1–3</sup> Selenium supplementation or consumption of low doses has many health benefits to human beings, among which the prevention of cancer and cardiovascular disease is of special interest to most scientists.<sup>1,3</sup> The biological properties of organic selenium are usually associated with the effects of selenium because in vivo selenium can be transformed into selenocysteine, part of the active center of the glutathione peroxidase (GSH-Px),<sup>1</sup> and selenium can also form selenoenzymes or selenopolysaccharides to exert an important role in maintaining the integrity of cellular membranes and protect the cellular lipids, lipoproteins, and DNA from oxidative damage.<sup>4</sup> For this reason, the selenium content in natural foods is drawing the attention of researchers and consumers, and selenium consumption is very popular in dietary supplements and functional foods.

It is widely recognized that the amount of selenium available in food resources depends on the agricultural species and the soil selenium content.<sup>5</sup> Ziyang green tea is a specific variety of selenium-enriched *Camellia sinensis* L. and is widely distributed in the second seleniferous region (Ziyang county) in China. Ziyang green tea as a selenium-enriched food has been popularly consumed in China for many years because it has been claimed to promote health and alleviate the severity of

many disorders.<sup>2</sup> Indeed, the selenium-enriched green tea has been shown to exhibit significantly higher antioxidant activities than the corresponding selenium-free green tea.<sup>6–9</sup> Recently, selenium-enriched green tea particles have also been found to inhibit the growth of human hepatoma cancer cells (HepG2), human adenocarcinoma of the lung cancer cells (A549), and human gastric cancer cells (MGC803).<sup>10</sup> For this reason, selenium-enriched Ziyang green tea is being increasingly produced in China and has been sold around the world.<sup>6</sup>

The growing interest in the nutritional prevention of cancer has prompted the identification of specific dietary constituents present in green tea with chemotherapeutic properties.<sup>11</sup> Traditionally, lipophilic flavonoids of green tea are recognized as the main ingredients responsible for its putative healthy benefits. However, it should be noted that tea is traditionally prepared using boiling water or decoction, and this preparation can leach the majority of water-soluble polysaccharides instead of flavonoids. Although tea polysaccharides have been reported to have wide bioactivities, such as immunomodulation, anticancer, antiradiation, antiblood coagulation, anti-HIV, and hypoglycemia,<sup>12–14</sup> the characteristics and antitumor activity of Ziyang green tea polysaccharides had not been studied.

Therefore, this study is designed to determine the cell growth inhibition of Se-GTPs, derived from a new source of the selenium-enriched Ziyang green tea, examine its effect on cell cycle and apoptosis in human breast cancer, and elucidate the possible antitumor mechanisms. In this study, we employed the human breast cancer MCF-7 cell line to assess the cell viability,

**Received:** August 25, 2012

**Revised:** December 26, 2012

**Accepted:** December 28, 2012

**Published:** December 28, 2012

cell cycle distribution, apoptosis, and changes in the protein levels involved in the control of cell cycle and apoptosis, including the expression of Bax and Bcl-2 and the activation of the caspase cascade. Furthermore, we also elucidated the possible involvement of ROS in the antitumor activity of the promising bioactive polysaccharides.

## MATERIALS AND METHODS

**Materials and Reagents.** 3-(4,5-Dimethylthiazol-2-yl)-2,5-diphenyltetrazolium bromide (MTT), dimethyl sulfoxide (DMSO), ribonuclease A (RNase-A), glycine, dodecyl sulfate sodium salt (SDS), phenylmethanesulfonyl fluoride (PMSF), ethylenediaminetetraacetic acid (EDTA), tris(hydroxymethyl)aminomethane hydrochloride (Tris-HCl), bovine serum albumin (BSA), nonfat milk powder, and propidium iodide (PI) were purchased from Sigma-Aldrich (St. Louis, MO, USA). The primary monoclonal antibodies against Bax and Bcl-2 and the horseradish peroxidase (HRP)-conjugated goat anti-mouse secondary antibody were obtained from BioVision, Inc. (BioVision, Milpitas, CA, USA). The monoclonal antibodies to GDPAH, p53, and CDK2 and the horseradish peroxidase (HRP)-conjugated goat anti-rabbit secondary antibody were obtained from Cell Signaling Technology, Inc. (Beverly, MA, USA). The enhanced chemiluminescence kit for HRP was purchased from Pioneer Technology, Inc. (Pioneer Technology, USA). Deionized water was prepared using a Millipore Milli Q-Plus system (Millipore, Bedford, MA, USA). All other chemicals were of the highest grade available.

**Extraction of Se-GTPs.** Fresh tea leaves plus buds of Ziyang tea cultivar were harvested in June 2011 from Ziyang County of Shaanxi Province, China, and were authenticated by Professor Xianhua Tian, College of Life Sciences, Shaanxi Normal University, China. Voucher specimens of the tea materials were deposited at the Key Laboratory of Ministry of Education for Medicinal Resource and Natural Pharmaceutical Chemistry, Shaanxi Normal University. The fresh tea leaves were air- and oven-dried at 45 °C until a constant weight (200 g). All of the tea was milled into a powder using a grinder (LX-04, Xi'an Jinzhen Machinery Co., Ltd. China), and the powder was extracted with distilled water (1:20, w/v) under reflux condition for 2 h in an 80 °C water bath. After three cycles, the solution was filtered and concentrated to 10% of the original volumes with a rotary evaporator under reduced pressure, and subsequently, 4 volumes of 95% (v/v) ethanol was added slowly by stirring to precipitate the polysaccharides. The resultant polysaccharide sediment was further refined by dissolution and precipitation three times. The refined polysaccharide pellets were dissolved completely in an appropriate volume of distilled water and dialyzed for 2 days against distilled water (cutoff MW 8000 Da). The retentate portion was deproteinized by a freeze-thaw process (FD-1, Henan Yuhua Instrument Co., China), which was repeated eight times, and then followed by filtration. Finally, the filtrate was lyophilized to yield brownish water-soluble polysaccharides (Se-GTPs).

**Chemical Analysis of Se-GTPs.** The carbohydrate content of the green tea polysaccharides was determined according to the phenol-sulfuric acid (H<sub>2</sub>SO<sub>4</sub>) method using glucose as the standard.<sup>15</sup> The quantification of uronic acid was performed according to the vitriol-carbazole method using glucuronic acid as the standard,<sup>16</sup> and proteins in the polysaccharides were quantified according to the Bradford method using bovine serum albumin (BSA) as the standard.<sup>17</sup> Monosaccharide composition analysis of the Se-GTPs was performed by a well-validated powerful HPLC-UV technique in our previous work.<sup>18</sup> Briefly, Se-GTPs was hydrolyzed into component monosaccharides with 2.0 M trifluoroacetic acid at 100 °C for 6 h and then labeled with 1-phenyl-3-methyl-5-pyrazolone (PMP), and subsequently the analysis of PMP-labeled monosaccharides was carried out on a Shimadzu LC-2010A HPLC system equipped with a quaternary gradient pump unit and an UV-vis detector (190–700 nm). The analytical column used was an RP-C<sub>18</sub> column (4.6 mm i.d. × 250 mm, 5 μm, Venusil, USA). Mobile phase A consisted of acetonitrile, and mobile phase B was 0.045% KH<sub>2</sub>PO<sub>4</sub>–0.05%

triethylamine buffer (pH 7.0) using a gradient elution of 95–95–90–90% B by a linear decrease from 0 to 5–8–30 min. The elution was carried out at a flow rate of 1.0 mL/min at 35 °C, and the wavelength for UV detection was 250 nm.

Selenium contents of tea powder and Se-GTPs were analyzed by double-channel atomic fluorescence spectrometry (AFS-810, Beijing Titan Instrument Co., Ltd.) as described previously.<sup>2</sup> Briefly, the samples were digested with 20 mL of a mixed solution of HNO<sub>3</sub> and HClO<sub>4</sub> (v/v, 4:1) at 170–175 °C for 60 min. After the mixture had cooled to room temperature, 10 mL of concentrated HCl was added to reduce Se<sup>6+</sup> to Se<sup>4+</sup> for an additional 30 min. The resultant solution was diluted with deionized water to 50 mL, containing 4 mL of concentrated HCl and 2 mL of 10% (w/w) K<sub>3</sub>Fe(CN)<sub>6</sub>.

**Cell Lines and Cell Culture.** Human breast carcinoma MCF-7 cells were obtained from Cell Bank of Institute of Biochemistry and Cell Biology, Chinese Academy of Sciences (Shanghai, China). MCF-7 cells and normal cells were grown in Dulbecco's modified Eagle's medium (DMEM)/low glucose (1.0 g/L) fluid medium (HyClone Laboratories, Inc., Novato, CA, USA), supplemented with L-glutamine (4.0 mM), sodium pyruvate (10 mM), 10% heat-inactivated fetal bovine serum (FBS), 100 units/mL of penicillin, and 100 μg/mL streptomycin at 5% CO<sub>2</sub> and in humidified 95% air.

**Analysis of Cell Viability.** Colorimetric MTT assay was performed to assess cell viability.<sup>19–21</sup> Briefly, cells (1 × 10<sup>5</sup>) were seeded in 96-well plates. After 24 h, the cells were treated with serial concentrations of Se-GTPs (0, 50, 100, 250, and 500 μg/mL) and fluorouracil (5-Fu, 100 μg/mL) for various periods (24 and 48 h). After the exposure period, 10 μL of MTT (5 mg/mL) in physiological buffered saline (PBS) solution was added to each well at a final concentration of 0.5 mg/mL, and then the plate was further incubated for 4 h. MTT-containing media were removed, and 150 μL of a solution containing 10% SDS plus 0.01 M HCl and 5% isobutyl alcohol was added to each well and mixed thoroughly to dissolve the formed crystal formazan. After incubation overnight at 37 °C to ensure that all crystals were dissolved, light absorption was measured at 570 nm using an enzyme-linked immunosorbent assay reader (Rayto-RT6000, Guangdong, China). Viability was expressed as a percentage of absorbance values in treated cells relative to that in control cells.

**Assay for Lactate Dehydrogenase (LDH).** The cytotoxic effects of Se-GTPs on the cultured cancer cells were determined by measuring LDH enzyme leakage from the cytosol of damaged cells into the medium, an indicator of irreversible cell death due to cell membrane damage.<sup>21</sup> An LDH kit (Jiancheng BioEngineering, Nanjing, China) was used to determine cellular membrane damage in response to Se-GTPs treatments as outlined by the manufacturer with minor modifications. Briefly, at the end of the incubation with the different treatments, 20 μL of culture medium was removed for extracellular LDH analysis. Each sample was detected, and the absorbance was read at a wavelength of 450 nm. The results were expressed as the enzymatic activity (U/L) present in culture media of Se-GTPs-treated cells versus control cells.

**Morphological Evaluation.** MCF-7 cells were incubated in a 6-well plate for 24 h at a density of 1 × 10<sup>5</sup> cells/well. After treatment with various doses of Se-GTPs for 48 h, the cells were washed with PBS. Nuclei staining with Hoechst-33258 was performed to investigate morphological changes. The cells were subsequently washed with PBS and fixed in 4% paraformaldehyde for 30 min at room temperature and then washed again with PBS. The fixed cells were incubated with Hoechst (50 μg/mL) for 20 min at room temperature in the dark. Stained solution was washed out, and the cells were visualized with a fluorescence microscope (Leica DMIL LED, Leica, Germany) for determination of nuclear morphological changes.

**Flow Cytometric Analysis of DNA Content for Cell Cycle.** MCF-7 cells were seeded in 6-well flat-bottom plates, grown overnight to achieve 90% confluence, and then treated with Se-GTPs (0, 100, and 500 μg/mL) for 24 h. After treatment, the detached cells in the medium were collected and combined with the remaining adherent cells that were detached by brief trypsinization (0.25% trypsin-EDTA, Sigma-Aldrich) at 37 °C for 5 min. The cells were fixed with cold 70% ethanol, stored at –20 °C for at least 24 h, and subsequently subjected

to PI staining (PI/RNase Staining Buffer); the cells were analyzed by flow cytometry (FACSCalibur, Becton Dickinson, Franklin Lakes, NJ, USA). CellQuest software (Becton Dickinson) was used to calculate the percentage of cells in G0/G1, S, and G2/M phases.<sup>19,21</sup>

**Apoptosis Assay.** MCF-7 cells were treated with Se-GTPs (0, 100, and 500  $\mu\text{g}/\text{mL}$ ) or fluorouracil (5-Fu, 100  $\mu\text{g}/\text{mL}$ ) for 48 h, and apoptotic cells were quantified by annexin V-FITC/PI double-staining assay. Early and late apoptotic changes in different cells were determined using an Annexin V-FITC/PI Apoptosis Detection Kit (BestBio, Shanghai, China) following the manufacturer's instruction.<sup>19,21</sup> Briefly, cells ( $1 \times 10^6$ ) were collected and washed twice with PBS and suspended in 400  $\mu\text{L}$  of binding buffer (containing 5  $\mu\text{L}$  of annexin V-FITC and 10  $\mu\text{L}$  of PI). Thereafter, the samples were incubated in the dark for 10 min at 4 °C and then analyzed on the flow cytometer (excitation, 488 nm; emission, 525 nm; FACSCalibur, Becton Dickinson). The number of annexin V-FITC-positive and PI-positive of cells in each field was determined by counting the cells directly.

**Measurement of Intracellular ROS.** The cultured MCF-7 cells at a density of  $1 \times 10^5$  cells were initially plated in 6-well plates for 24 h. The cells were then preincubated with or without Se-GTPs (0, 100, and 500  $\mu\text{g}/\text{mL}$ ) or  $\text{H}_2\text{O}_2$  (10  $\mu\text{M}$ ) as positive control. After 12 h, the cells were subsequently washed twice with PBS. The treated cells were further incubated with 10  $\mu\text{M}$  dichlorofluorescein diacetate probe (DCFH-DA, Jiancheng BioEngineering, Nanjing, China) at 37 °C for 30 min. The DCFH fluorescence intensity of the cells was quantified with flow cytometry (excitation, 488 nm; emission, 525 nm), and the results were given as percentages relative to the fluorescence of the control cells (100%).<sup>21</sup>

**Western Blot Analysis.** MCF-7 cells ( $5 \times 10^5$ ) were plated in a 25  $\text{cm}^2$  cell culture flask. After 24 h, the cells were treated with PBS vehicle alone or Se-GTPs at 100 and 500  $\mu\text{g}/\text{mL}$  for 24 or 48 h, respectively, and the cells were collected and lysed with 0.1 mL of cold lysis buffer (150 mM NaCl, 50 mM of pH 7.4 Tris, 1 mM EDTA, 1% Triton X-100, 0.5% SDS, 0.01% PMSF). The cell lysate was centrifuged at 12000g for 30 min at 4 °C. Protein concentrations were determined with a BCA protein assay kit (BestBio, Shanghai, China) using bovine serum albumin as the standard. Equal amounts of cell lysate proteins (50  $\mu\text{g}$ ) were mixed with a one-fourth volume of 5 $\times$  loading buffer and boiled for 5 min, followed by electrophoresis using SDS-PAGE for 90 min at 110 V. The separated proteins were transferred to polyvinylidene difluoride membrane for 2 h at 300 mA for assessment of the levels of Bax, Bcl-2, CDK2, p53, and GAPDH. After nonspecific binding sites were blocked with 5% nonfat dry milk in PBS for 60 min, the transferred membrane was incubated at 4 °C overnight with primary antibodies at the following concentrations: mouse anti-Bax, 1:500; mouse anti-Bcl-2, 1:500; rabbit anti-CDK2, 1:500; rabbit anti-p53, 1:500; and rabbit anti-GAPDH, 1:1000. The membrane was extensively washed by PBST (0.1% Tween-20 in PBS buffer), followed by incubation with horseradish peroxidase-conjugated goat anti-mouse or -rabbit secondary antibody (1:5000) for 2 h. Proteins of interest were incubated with ECL detection reagent (Pierce) and developed by exposure to X-ray films. The protein expression was quantified densitometrically using ImageJ software (version 1.43, National Institutes of Health, Bethesda, MD, USA).<sup>19,22,23</sup>

**Assay for Caspase-3 and -9 Activities.** The assay is based on the ability of the active enzyme to cleave the chromophore from the enzyme substrate Ac-LEHD-pNA for caspase-9 and Ac-DEVD-pNA for caspase-3.<sup>19,24,25</sup> Caspase-3 and -9 activities were assessed according to the manufacturer's instruction of the caspase colorimetric kit (BestBio Inc.). MCF-7 cells were seeded in 6-well cell culture plates at an initial density of  $5.0 \times 10^6$  cells and treated with different concentrations of Se-GTPs (0, 100, and 500  $\mu\text{g}/\text{mL}$ ) for 48 h. The cells were harvested and lysed for 10 min in 50 mL of lysis buffer, which contained 2 mM DTT. After centrifugation, the supernatant containing 100 mg of protein was incubated with caspase-3 substrate (Ac-DEVD-pNA) and caspase-9 substrate (Ac-LEHD-pNA) in reaction buffer, respectively. All samples were incubated in 96-well flat-bottom microplates at 37 °C for 2 h. Levels of released pNA were

measured at OD 405 nm with an ELISA reader (Rayto-RT6000, Guangdong, China).<sup>19,24,25</sup>

**Statistical Analysis.** All determinations were performed in triplicate, and data were expressed as the mean  $\pm$  SD.  $\text{IC}_{50}$  values were calculated by regression analysis. The data were subjected to an analysis of variance (ANOVA,  $p < 0.05$ ), and Duncan's multiple-range tests (SPSS, version 13.0). A significant difference was judged to exist at a level of  $p < 0.05$ .

## RESULTS

**Chemical Properties of Se-GTPs.** Se-GTPs were extracted from Ziyang selenium-enriched green tea, and their total carbohydrate content and total uronic acid content were 62.4 and 16.3% (w/w), respectively. With this extraction, selenium content of Se-GTPs was 1.52  $\mu\text{g}/\text{g}$ , which was significantly higher than that of the original tea (0.57  $\mu\text{g}/\text{g}$ ), suggesting that Se-GTPs were selenium-containing conjugates because the small molecular selenium-free should be removed via dialysis processing (cutoff MW > 8000 Da) in the purification of the macromolecular polysaccharides. HPLC analysis showed that Se-GTPs were the typical heteropolysaccharides that consisted of mannose, ribose, rhamnose, glucuronic acid, galacturonic acid, glucose, xylose, galactose, arabinose, and fucose with the corresponding mole percentages of 4.3, 1.4, 4.1, 2.6, 3.0, 31.4, 4.6, 21.8, 23.5, and 3.3%, respectively (Figure 1A). As a result, Se-GTPs were shown to be a selenium-containing polysaccharide extract with high purity.

**Inhibition of Cell Proliferation in Se-GTPs-Treated MCF-7 Cells.** The effect of Se-GTPs on the growth of MCF-7 cells was investigated using the MTT assay. As shown in Figure 1B, Se-GTPs at all the tested concentrations of 50–500  $\mu\text{g}/\text{mL}$  significantly inhibited the growth of MCF-7 cells in a dose- and time-dependent manner ( $p < 0.05$  vs untreated cells). With the increase in concentrations of Se-GTPs ranging from 100 to 500  $\mu\text{g}/\text{mL}$ , the cell viability was sharply decreased, compared to control cells ( $p < 0.01$ ), where only 56.3, 45.4, and 28.7% cells survived from the treatment with Se-GTPs at 100, 250, and 500  $\mu\text{g}/\text{mL}$  for 48 h, respectively. It is worth noting that Se-GTPs exhibited high growth-inhibitory effects on MCF-7 cells, similar to those of the same concentration of 5-Fu (100  $\mu\text{g}/\text{mL}$ ,  $p > 0.05$ ). The value of  $\text{IC}_{50}$ , defined as the concentration at which the cell proliferation was inhibited by 50% of control cells, was 140.1  $\mu\text{g}/\text{mL}$ .

To further confirm the proliferation inhibitory effects of Se-GTPs on MCF-7 cells, the LDH assay was used to determine the effect of Se-GTPs on the LDH leakage of MCF-7, as an indicator of MCF-7 cytotoxicity. As shown in Figure 1C, treatment with Se-GTPs at concentrations of 50–500  $\mu\text{g}/\text{mL}$  for 48 h dose-dependently resulted in an increase in cytotoxicity, as reflected by the 3.86-, 5.60-, 6.68-, and 8.03-fold increases in LDH leakage from MCF-7 cells, respectively ( $p < 0.01$  vs control).

**Morphology Changes Induced by Se-GTPs.** As illustrated in Figure 2, MCF-7 cells showed a change in the morphology after treatment with Se-GTPs at 100 and 500  $\mu\text{g}/\text{mL}$ . As observed under a microscope, the morphology of the normal untreated cells was regular (image a), whereas cells treated with Se-GTPs exhibited morphological alterations, such as increased cell shrinkage and membrane blebings (images b and c). At the same time, some cells lost their ability to adhere to the plate surface, detached from the bottom, aggregated, and floated in the medium, leading to the decreased density of Se-GTPs-treated cells. The extent of the changes in cell



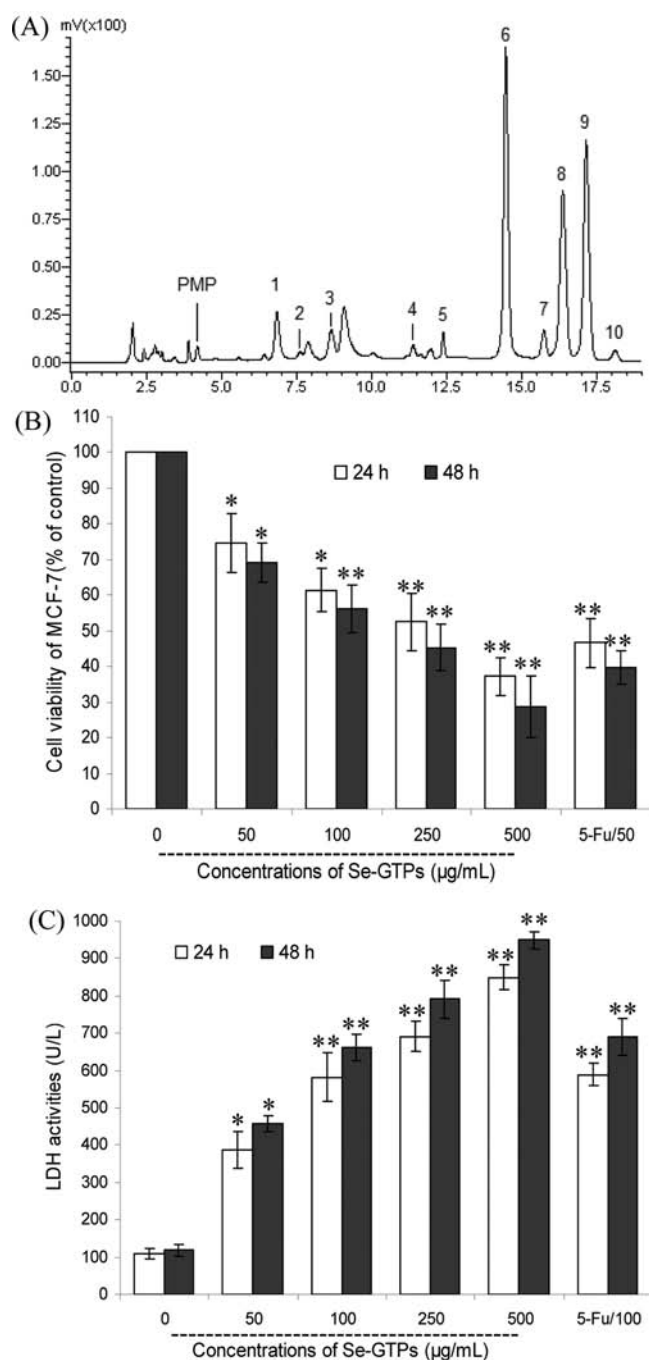


**Figure 1.** HPLC chromatograms of the component monosaccharides of Se-GTPs (A) and their antiproliferative effect and cytotoxicity on human breast cancer MCF-7 cells estimated by MTT assay (B) and LDH leakage analysis (C). Peaks: 1, mannose; 2, ribose; 3, rhamnose; 4, glucuronic acid; 5, galacturonic acid; 6, glucose; 7, xylose; 8, galactose; 9, arabinose; 10, fucose. MCF-7 cells were incubated with indicated concentrations of Se-GTPs (0, 50, 100, 250, and 500 µg/mL), and fluorouracil (5-Fu, 100 µg/mL) was used as positive control. After 24 or 48 h of treatment, cell proliferation was assessed by MTT assay and cytotoxic effect was measured by LDH assay. Each bar represents the mean  $\pm$  SD of three independent experiments. (\*)  $p < 0.05$  and (\*\*)  $p < 0.01$  indicate statistically significant differences versus control group.

morphology and density depended on the concentrations of Se-GTPs (Figure 2A). Furthermore, a DNA binding dye, Hoechst 33258, was also used for nuclear staining to elucidate

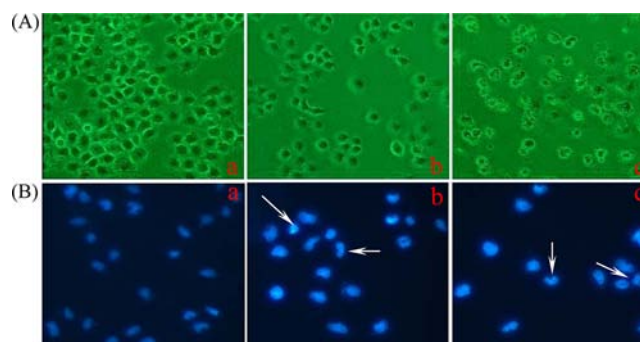


**Figure 2.** Effect of Se-GTPs treatment on the cell or nuclear morphological changes of MCF-7 cells. MCF-7 cells were treated with vehicle (image a, control) or Se-GTPs at 100 µg/mL (image b) or 500 µg/mL (image c) for 48 h. (A) The cells were observed microscopically (original microscope magnification, 200 $\times$ ). (B) The cells were dyed with Hoechst 33258 and visualized under fluorescence microscopically (original microscope magnification, 200 $\times$ ).

apoptotic cell death due to the exposure of MCF-7 cells to Se-GTPs (Figure 2B). Under a fluorescence microscope, the normal cells with nuclear staining exhibited intact and round-shaped nuclei, characterized by slight staining because of euchromatin in MCF-7 cells (image a). In contrast, the exposure to Se-GTPs at 100 and 500 µg/mL for 48 h altered the MCF-7 nuclear morphology with increased condensed or fragmental chromatin (images b and c), which is characteristic of apoptotic cells.<sup>26,27</sup>

#### ROS Accumulation in Se-GTPs-Induced MCF-7 Cells.

To determine whether intracellular ROS are involved in the cellular mechanism of growth inhibition by Se-GTPs on the MCF-7 cells, we employed flow cytometry to detect the changes of CM-H<sub>2</sub>DCFDA fluorescence intensity in MCF-7 cells exposed to Se-GTPs for 12 h. As depicted in Figure 3A, treatment with Se-GTPs increased the proportion of cells with higher green fluorescence intensity in a dose-dependent manner, indicating that Se-GTPs induced the accumulation of intracellular ROS in the MCF-7 cells. As displayed in Figure 3B, Se-GTPs at 100 µg/mL caused an 8.2-fold increase in ROS accumulation in MCF-7 cells, and 500 µg/mL of Se-GTPs led to a concentration-dependent increase of intracellular ROS by 12.4-fold, contrasted to untreated cells ( $p < 0.01$ ). A similar increase by 9.4-fold in green fluorescence intensity of MCF-7 cells was also obtained via the incubation with H<sub>2</sub>O<sub>2</sub> (10 µM) serving as a positive control for measuring the effects of oxidative stress (Figure 3A,  $p < 0.01$  vs control). These results indicate that Se-GTPs can induce growth inhibition and apoptosis through enhancing intracellular ROS oxidative stress of MCF-7 cancer cells.

#### Cell Cycle Arrest and Apoptosis Induction by Se-GTPs in MCF-7 Cells.

In cancer, there are fundamental alterations in the genetic control of cell division, resulting in an unrestrained cell proliferation, and therefore, induction of cell cycle arrest has been appreciated as a target for the management of cancer.<sup>28</sup> To estimate the effect of Se-GTPs treatment on the distribution of cells in the cell cycle, we performed DNA cell cycle analysis by flow cytometry. Figure 4A shows the effects of Se-GTPs on the cell cycle phase (G<sub>0</sub>/G<sub>1</sub>, S, and G<sub>2</sub>/M) distribution of MCF-7 cells with PI staining. The MCF-7 treatment with Se-GTPs at 100 and 500 µg/mL for 24 h induced a dose-dependent accumulation of cells in the G<sub>2</sub>/M phase from 5.7% of the control group to 19.7 and 34.3% ( $p <$

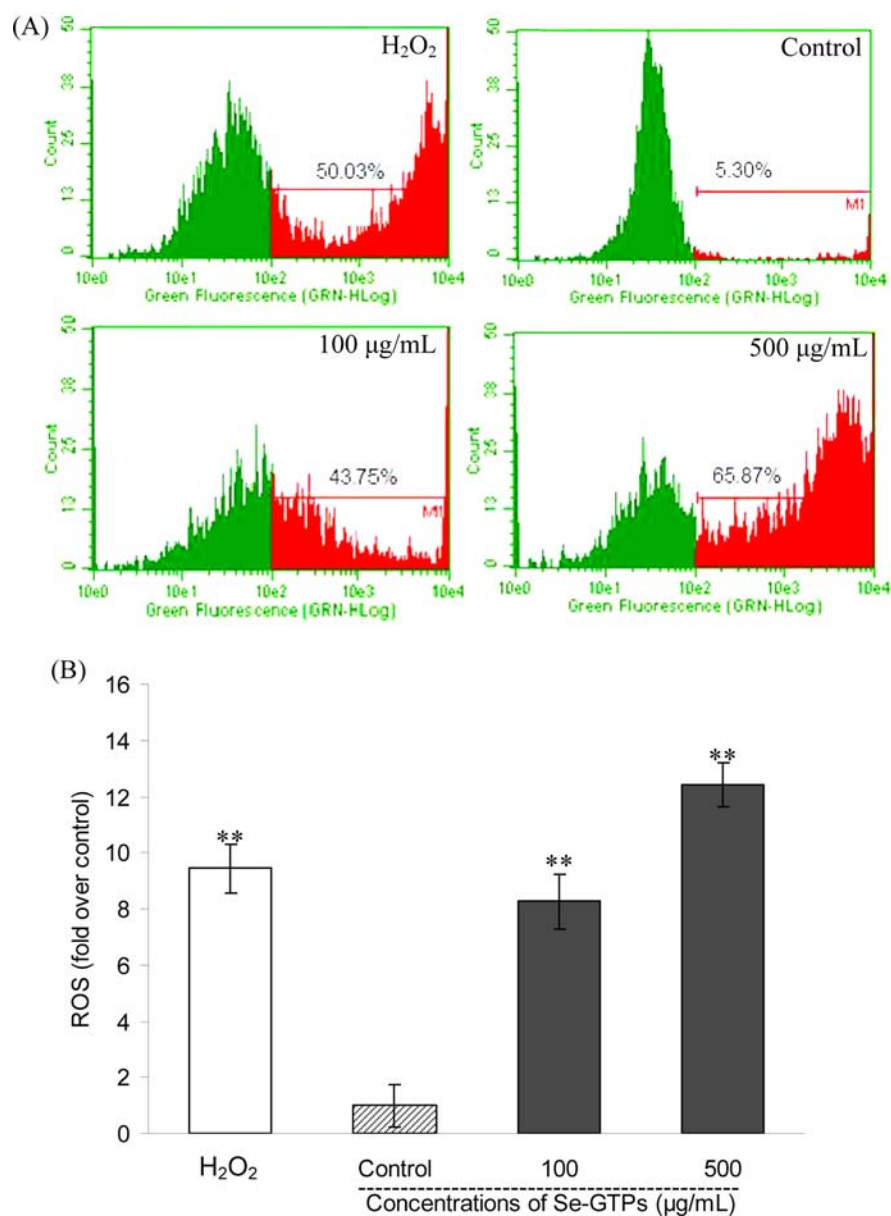


**Figure 3.** Se-GTPs-mediated accumulation of intracellular ROS in MCF-7 cells. MCF-7 cells were preincubated with or without various concentrations of Se-GTPs (0, 100, and 500  $\mu\text{g/mL}$ ) for 12 h, and then the intracellular ROS level was measured by DCFH-DA probe. 100  $\mu\text{M}$   $\text{H}_2\text{O}_2$  was used as positive control. The results represent the mean  $\pm$  SD of three independent experiments. (\*\*)  $p < 0.01$  indicates statistically significant difference with untreated cells.

0.05 or  $p < 0.01$ , Figure 4B,C), accompanied by a decrease in the percentage of cells in the G<sub>0</sub>/G<sub>1</sub> phase from 75.7 to 52.8 and 42.9%, respectively. At the tested concentrations, Se-GTPs did not induce significant change in the S phase (Figure 4C). The accumulation of sub-G<sub>1</sub> phase cells, a hallmark of apoptosis, was noted at 100  $\mu\text{g/mL}$  Se-GTPs treatment (Figure 4A, M1). These results suggest that Se-GTPs can inhibit the growth of MCF-7 cancer cells through cell cycle arrest in the G<sub>2</sub>/M phase.

Cell cycle deregulation and apoptosis are closely related events, and disruption of cell cycle progression may ultimately lead to apoptotic/necrotic death.<sup>25</sup> To further evaluate the effect of Se-GTPs on the induction of apoptosis, the MCF-7 cells were incubated with different concentrations of Se-GTPs, and then the cells were double stained with annexin V-FITC and PI, followed by quantitative flow cytometry analysis. As

shown in Figure 5A, after treatment with Se-GTPs for 48 h, the cells presented the feature of early apoptosis, and the feature appeared more frequently with increasing concentrations of Se-GTPs, suggesting that Se-GTPs induced apoptosis of MCF-7 cells. Compared with vehicle-treated cells, Se-GTPs caused 30.9 and 46.5% increases of the apoptotic cells including both the early and late apoptotic cells at concentrations of 100 and 500  $\mu\text{g/mL}$  after 48 h of treatment, respectively ( $p < 0.01$ , Figure 5B). These results indicate that Se-GTPs-induced apoptosis in MCF-7 cells is also likely to involve modulation of cell cycle progression.

**Examination of the Levels of Proteins Associated with Cell Cycle and Apoptosis.** The underlying mechanism of Se-GTPs-induced alteration of the protein profile involved in the cell cycle and apoptosis in the MCF-7 cells was further delineated by Western blotting assay and relatively quantitated

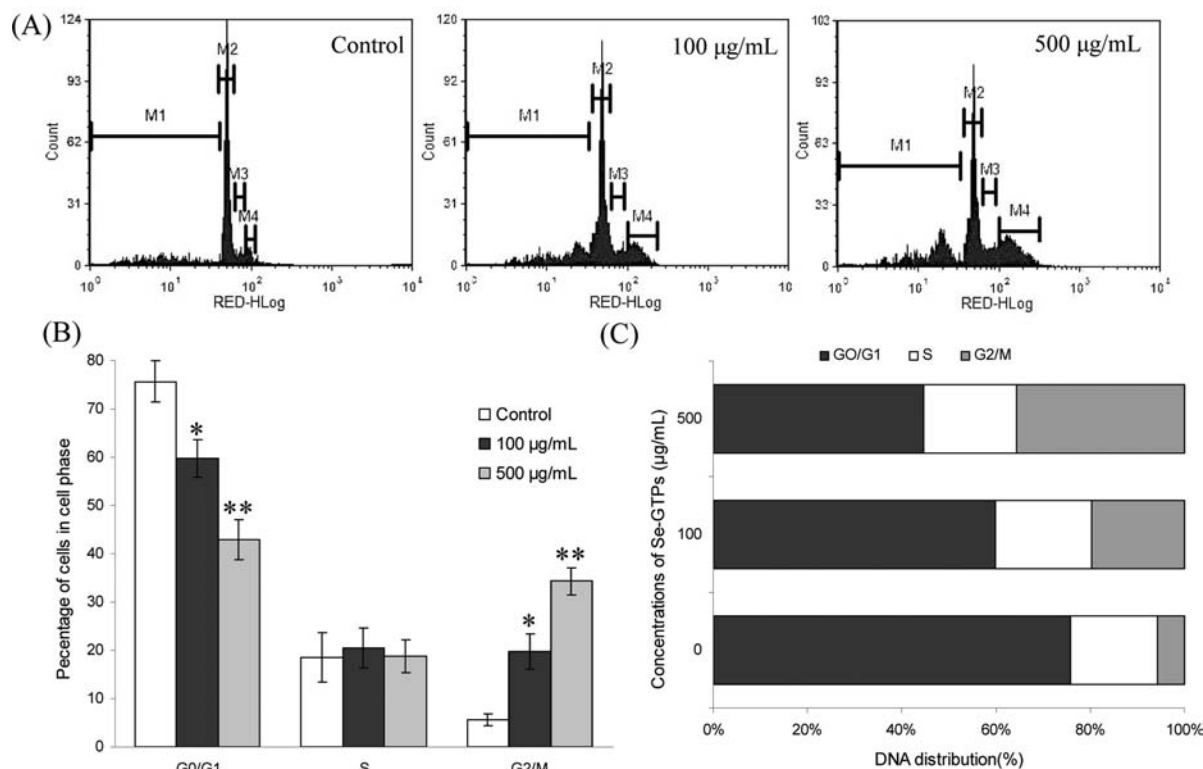


**Figure 4.** Cell cycle analysis of Se-GTPs-treated cells. MCF-7 cells were treated with Se-GTPs as indicated and then incubated at 37 °C for 24 h. The cells were harvested and fixed in 70% alcohol and then stained with propidium iodide. The stained cells were analyzed using a flow cytometer, and the distribution in each cell cycle phase was determined by CellQuest software (A). Markers M1, M2, M3, and M4 represent cells in sub-G1, G1, S, and G2 phases, respectively. Data are expressed as a percentage of total cells (B) and are expressed as the mean  $\pm$  SD of three independent experiments. The asterisk (\*) represents a significant difference as compared to untreated cells: (\*)  $p < 0.05$ ; (\*\*)  $p < 0.01$ .

by densitometric analysis. The levels of GAPDH served as an internal control. To determine whether Se-GTPs induced apoptosis by triggering the mitochondrial apoptotic pathway, we measured the change in the expression of the Bcl-2 family of proteins, which are key regulators of apoptosis and commonly overexpressed in many malignancies.<sup>30</sup> It was found that the expression of the antiapoptotic protein Bcl-2 was decreased whereas the apoptotic protein Bax was increased after the cells were treated with Se-GTPs, leading to an increase of the Bax/Bcl-2 ratio, which is crucial for the activation of the mitochondrial apoptotic pathway (Figure 6). As shown in Figure 6A, the treatment of Se-GTPs at 100 and 500 µg/mL for 48 h up-regulated the expression of Bax by 2.37- and 2.82-fold compared to the untreated cells ( $p < 0.05$ ), whereas the expression of Bcl-2 was highly down-regulated by 0.94- and 0.79-fold ( $p < 0.05$ ), respectively. When MCF-7 cells were incubated with 500 µg/mL of Se-GTPs for 24 and 48 h, the Bax expression significantly increased up to 1.31- and 1.39-fold above that in control cells, respectively ( $p < 0.05$ ), whereas BCL-2 expression was decreased 0.83- and 0.60-fold, with respect to the control cells ( $p < 0.05$ ), respectively.

As demonstrated in Figure 6B, the Bax/Bcl-2 ratio was sharply elevated up to 2.52- and 3.57-fold of untreated cells after 100 and 500 µg/mL Se-GTPs treatment for 48 h, respectively ( $p < 0.01$ ). When MCF-7 cells were incubated with 500 µg/mL of Se-GTPs for 24 and 48 h, the ratio of Bax/Bcl-2 was also markedly enhanced up to 1.58- and 2.32-fold of untreated cells, respectively ( $p < 0.01$ , Figure 6C). We next examined the effect of Se-GTPs on cell cycle regulatory molecules of p53 and CDK2. As can be seen in Figure 6A, the

treatment of MCF-7 cells with Se-GTPs resulted in up-regulation in the level of p53 protein, which is responsible for cell cycle progression in the G2/M phase.<sup>31</sup> However, the level of CDK2 protein, which regulates S phase entry from the late G1 phase,<sup>32</sup> remained unchanged ( $p > 0.05$  vs untreated cells) following the treatment.

**Effects of Se-GTPs on the Caspase-9 and -3 Activities in MCF-7 Cells.** Caspase activation represents the irreversible or execution stage of apoptosis.<sup>33</sup> To further examine the involvement of caspases in apoptosis induction of Se-GTPs, the activities of caspase-3 and caspase-9 were also examined as shown in Figure 7. It was found that caspase-3 and caspase-9 were both activated significantly after Se-GTPs treatment for 48 h in MCF-7 cells. In MCF-7 cells, incubated with 100 µg/mL Se-GTPs, caspase-3 and -9 activities were markedly increased by 70.69 and 47.63% ( $p < 0.01$ ), and the higher concentration (500 µg/mL) further enhanced the activation by 130.37 and 105.70% above control cells ( $p < 0.01$ ), respectively. This finding indicates that the mitochondrial pathway is involved in Se-GTPs-induced apoptosis.

## DISCUSSION

The fundamental importance of selenium ingestion to human health has received considerable attention. Selenium from a variety of sources, such as yeast, green tea, algae, and edible mushrooms, is incorporated into proteins or polysaccharides as organic selenium compounds with high bioavailability, high retention, and low toxicity to the body and are considered to be better sources of selenium than inorganic selenium compounds.<sup>1,3-5</sup> Previous studies confirmed that some extracts of

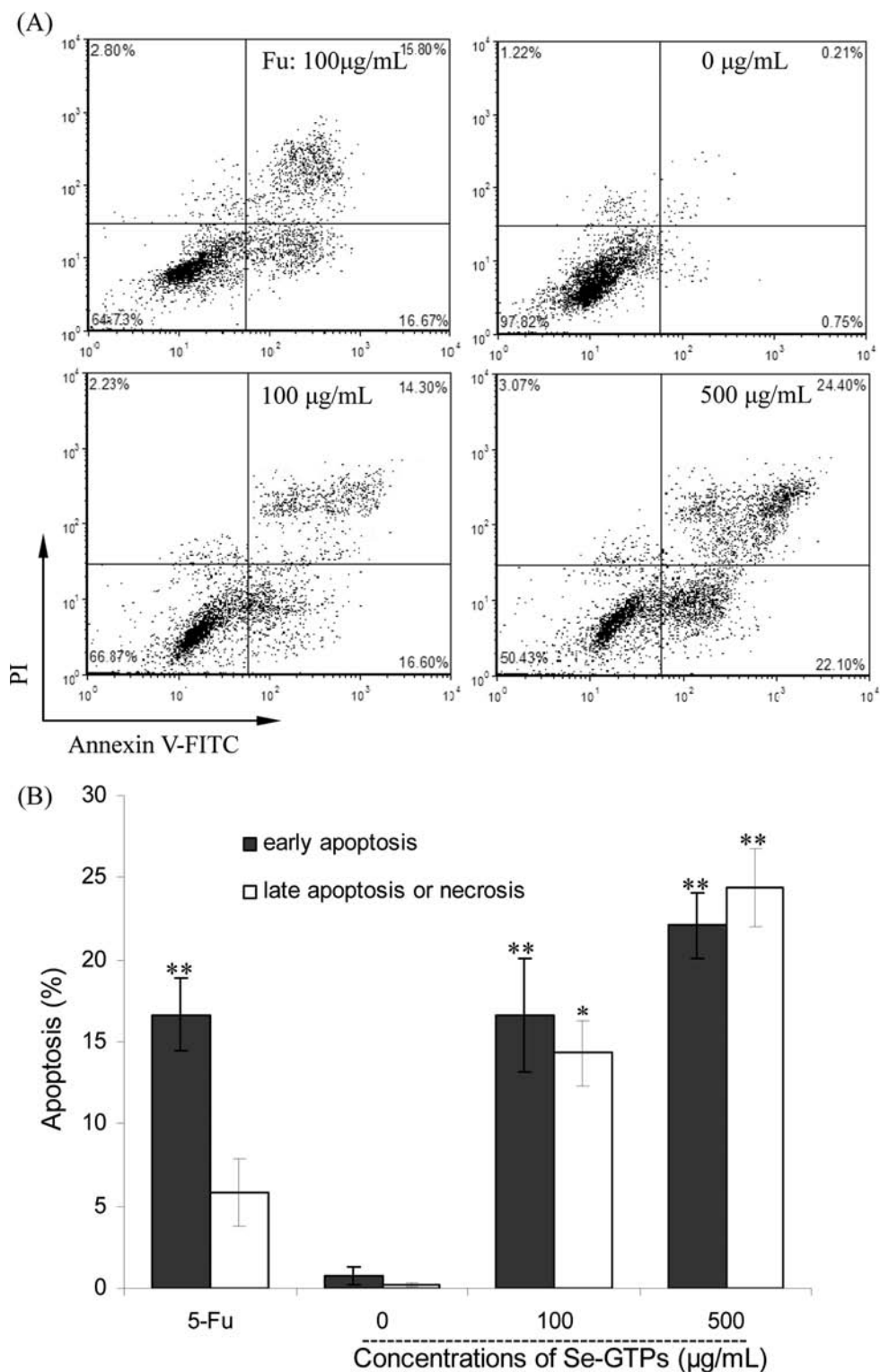


**Figure 5.** Quantitative analysis of apoptotic cells induced by Se-GTPs using annexin V/PI double-staining assay. MCF-7 cells were treated with Se-GTPs (100 and 500  $\mu\text{g/mL}$ ) for 48 h. After harvesting, MCF-7 cells were double-stained with annexin V-FITC and PI, and then 10000 cells were analyzed by flow cytometry. All experiments were done independently in triplicate per experimental point, and representative dot plots of annexin V-FITC/PI staining are shown. (\*\*)  $p < 0.01$  indicates statistically significant difference with untreated cells.

selenium-containing proteins or polysaccharides exhibited high antitumor activity.<sup>10</sup> At the same time, natural plant polysaccharides have gained interest as nontoxic chemopreventive or chemotherapeutic agents capable of inducing tumor cell death in a variety of cancer types.<sup>34</sup> Breast cancer is known to be the most common malignancy and the second

leading cause of cancer mortality in women in both developed and developing countries.<sup>35,36</sup> The present study is the first to show that selenium-enriched polysaccharide extract Se-GTPs inhibited the growth of human breast adenocarcinoma MCF-7 cells. We also characterized the mechanisms by which Se-GTPs exerted their inhibitory effects on human breast cancer MCF-7



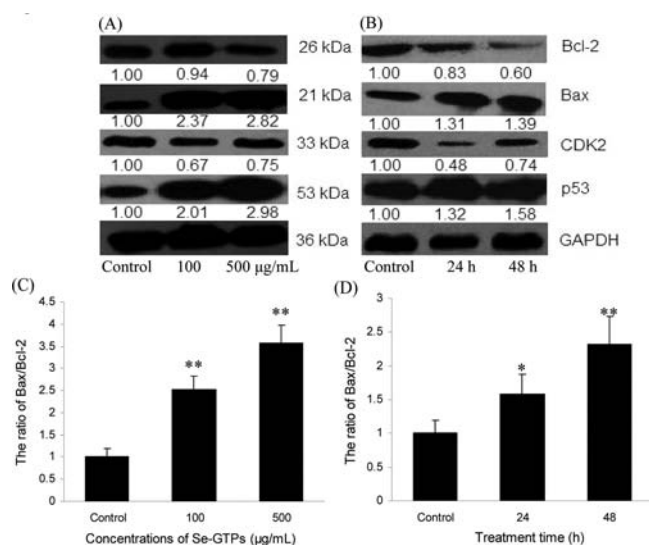


**Figure 6.** Effects of Se-GTPs on the expression of proteins associated with cell cycle and apoptosis in MCF-7 cells. MCF-7 cells were treated with Se-GTPs at 100 and 500  $\mu\text{g/mL}$  for 48 h (A) and at 500  $\mu\text{g/mL}$  for 24 and 48 h (B), and the corresponding ratio of Bax/Bcl-2 is shown (C, D), respectively. Western blot analysis was performed in triplicate per experimental point, and the relative expression of protein was quantified densitometrically; GAPDH was used as reference control. The number under each band in the immunoblot indicates the relative intensity of the corresponding band. (\*)  $p < 0.01$  as compared with the control cells.

cells by inducing G2/M cell cycle arrest and undergoing apoptosis in a dose- and time-dependent manner.

This research has demonstrated that treatment with various concentrations of Se-GTPs could profoundly inhibit the cell proliferation of MCF-7 cells, and the inhibitory effect was further confirmed by the assay of LDH enzyme leakage from the cytosol of damaged cells into the medium, an indicator of irreversible cell death due to cell membrane damage.<sup>21,37</sup> It is well-known that inhibition of tumorigenesis often involves modulation of the signal transduction pathway, leading to cell cycle arrest and, consequently, apoptosis.<sup>28,38</sup> The eukaryotic cell cycle is strictly regulated by complexes containing CDKs and cyclins, which are critical for the progression of cell cycle and the inactivation of which leads to cell cycle arrest; therefore, induction of cell cycle arrest has been appreciated as a target for the management of cancer.<sup>28,38</sup> Our results suggest that Se-GTPs block proliferation of tumor cells by arresting the cells in the G2/M phase of the cell cycle. It is also widely recognized that up-regulation of p53 and p21 proteins leads to an inhibition of growth and proliferation in cancer cells, and the increase in levels of p21, a key downstream target of p53 and one of the cyclin-dependent kinase inhibitors, mediates both G1 and G2/M phase arrest.<sup>31</sup> In this study, treatment of MCF-7 cells with Se-GTPs resulted in a significant up-regulation in the expression level of p53 protein (Figure 6A), whereas the level of CDK2 protein, which regulates the G0/S phase, remained unchanged following the intervention. Thus, we suggest that the growth inhibition of Se-GTPs is associated with the G2/M arrest, which is implicated in p53-dependent regulation in MCF-7 cells.

Mitochondria is thought to be key pathway for apoptosis, and mitochondrial function is regulated through Bcl-2 family proteins comprising antiapoptotic (Bcl-2, Bcl-XL) and proapoptotic members (Bax, Bak).<sup>20,25,30</sup> In this study, Se-

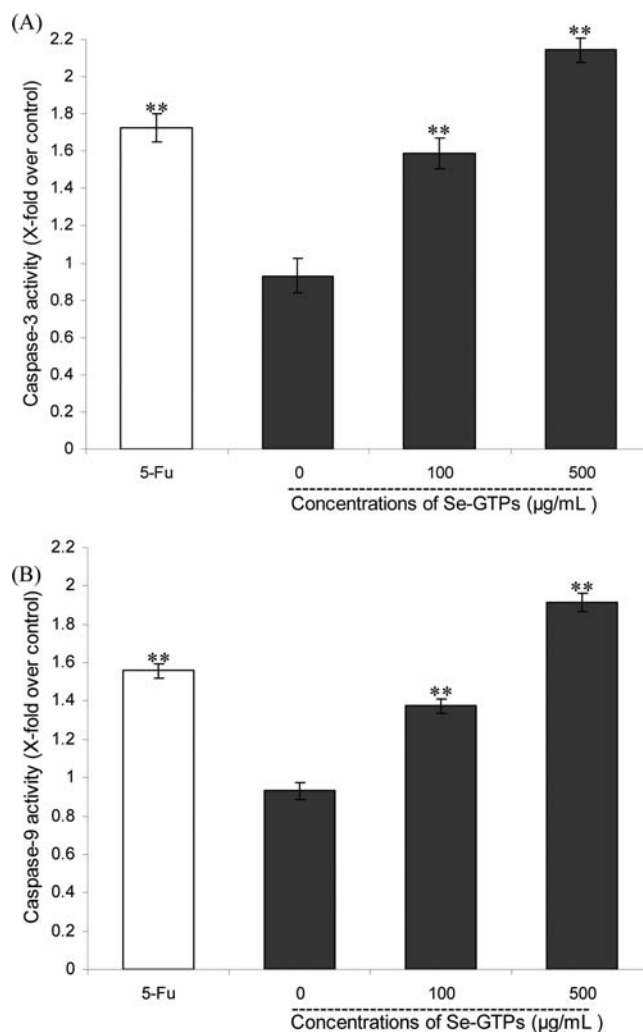


**Figure 7.** Effects of Se-GTPs on the activities of caspase-3 (A) and caspase-9 (B) in the MCF-7 cells. Values of optical density (OD) at 405 nm were determined by an ELISA reader. Values are the mean  $\pm$  SD of three independent experiments. (\*\*\*)  $p < 0.01$  versus untreated cells.

GTPs treatment resulted in a significant increase of Bax expression and a decrease of Bcl-2, suggesting that changes in the ratio of proapoptotic and antiapoptotic Bcl-2 family proteins might contribute to the apoptosis promotion of Se-GTPs (Figure 8). There is mounting evidence that the ratio of Bax and Bcl-2, and not Bcl-2 alone, plays a decisive role, especially during the occurrence of drug-induced apoptosis.<sup>38–40</sup> In addition, it is becoming appreciated that p53, most closely related to the tumor suppressor gene, serves as a key player in a variety of extracellular and intracellular regulation of DNA repair, cell cycle arrest, and induction of apoptosis,<sup>31,39,40</sup> exerting its function mainly through transcriptional activation of target genes, such as the cyclin-dependent kinase (CDKs) inhibitor p21, for the cell cycle arrest and the proapoptotic protein Bax for inducing apoptosis.<sup>39,40</sup> It is also reported that tumor suppressor protein p53 can directly activate Bax, which is involved in the regulation of apoptosis.<sup>39</sup> Herein, our study demonstrated that Se-GTPs could enhance p53 protein expression, suggesting that p53 was involved in apoptosis regulation of Se-GTPs (Figure 8).<sup>31,40</sup> Moreover, caspases are a family of cysteine proteases that play a central role during the execution phase of apoptosis.<sup>41</sup> Particularly, caspase-3 has



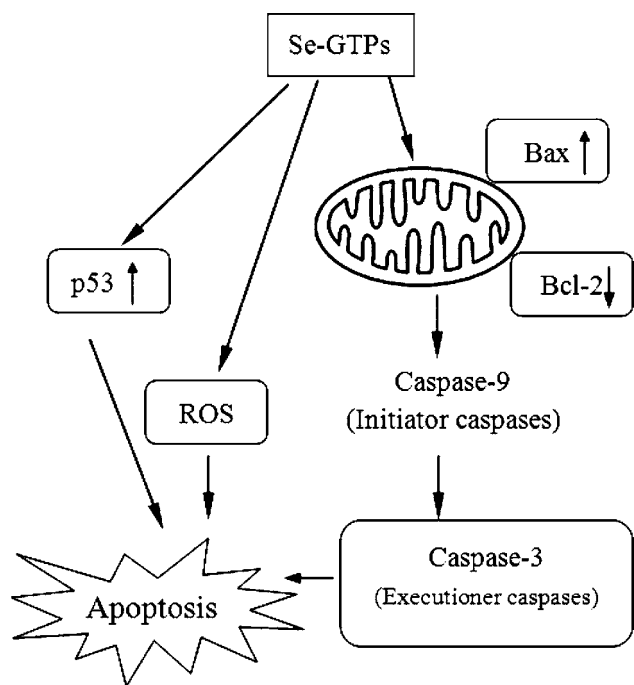


**Figure 8.** Proposed possible signal pathways for Se-GTPs-induced apoptosis in human breast cancer MCF-7 cells.

been shown to play a central role in the terminal and execution phase of apoptosis as well as by other activated caspases, such as caspase-8 and caspase-9, in response to proapoptotic signals.<sup>42</sup> To explore whether Se-GTPs induce apoptosis by activation of caspases, caspase-3 and -9 activities were detected. The results shown in Figure 7 clearly confirmed that caspase-3 and caspase-9 were activated in MCF-7 cells after Se-GTPs treatment. The morphology changes of Se-GTPs-treated cells were typical of apoptosis, nuclear condensation, DNA fragmentation (Figure 2), and caspase activation, all hallmarks of apoptosis. These results suggest that Se-GTPs increase caspase activities through the regulation of Bcl-2 family protein (Figure 8),<sup>30</sup> and these occurrences of mitochondrial apoptotic events play an important role in Se-GTPs-mediated apoptosis.

Mitochondria is a source of ROS during apoptosis,<sup>43</sup> and some natural phytochemicals have been shown to stimulate the cellular oxidative metabolism, which can reduce mitochondria membrane potential, leading to increased generation of ROS and apoptosis.<sup>26,43</sup> ROS has been implicated as a second messenger in multiple signaling pathways and can also play an important role in apoptosis by regulating the activity of certain enzymes involved in the cell death pathway.<sup>43</sup> Evidence is accumulating which indicates that many chemotherapeutic agents may be selectively toxic to tumor cells because they increase oxidative stress and enhance these already stressed cells beyond their limit.<sup>44</sup> To further investigate the proapoptotic effects of Se-GTPs on mitochondria, the level of intracellular ROS in MCF-7 cells was measured in the present study. Here, we showed for the first time the generation of mitochondrial ROS in MCF-7 cells exposed to Se-GTPs, indicating that ROS production led to apoptotic cell death via the mitochondrial pathway (Figure 8). Our results are in agreement with previous studies that pointed out ROS as secondary messengers in apoptosis provoked by anticancer agents, such as resveratrol and curcumin.<sup>27</sup> These results suggest that Se-GTPs-mediated ROS generation represents the

central trigger for activation of the apoptotic cascade. Exposure of MCF-7 cells to Se-GTPs resulted in the generation of ROS and up-regulation of p53, an elevation of Bax, and a reduction of Bcl-2. The movement of Bax to the mitochondria reduces the mitochondrial membrane potential, an event that results in an activation of caspase-3 and caspase-9, and leads to apoptotic changes (Figure 8).<sup>45</sup> This observation is consistent with the conclusion of a recent study about the effect of capsaicin in colorectal cancer colo 205 cell lines.<sup>45</sup>

In conclusion, this is the first study to show that a selenium-enriched polysaccharide extract Se-GTPs, derived from Ziyang selenium-enriched green tea, could inhibit the proliferation of human breast cancer MCF-7 cells. The cellular mechanism responsible for the inhibitory effect of Se-GTPs on MCF-7 cancer cells involves cell cycle arrest in the G2/M phase. Se-GTPs-induced apoptosis mediated by ROS generation and the up-regulation of p53, an elevation of Bax, and a reduction of Bcl-2, followed by activation of caspase-3 and caspase-9, was demonstrated. These findings may aid in the understanding of the mode of tumor-inhibitory action of Se-GTPs and provide a theoretical basis for the prevention or treatment of human breast cancer with tea polysaccharide extract.

## ■ AUTHOR INFORMATION

### Corresponding Author

\*Phone: +86-29-85310517. Fax: +86-29-85310517. E-mail: xbyang@snnu.edu.cn.

### Funding

This work was supported by the National Natural Science Foundation of China (C30972054, C31171678), a grant from Innovation Funds of Graduate Programs of Shaanxi Normal University (2012CXS051), and the Fundamental Research Funds for the Central Universities of Shaanxi Normal University, China (GK201103004).

### Notes

The authors declare no competing financial interest.

## ■ REFERENCES

- (1) Sanmartin, C.; Plano, D.; Sharma, A. K.; Palop, J. A. Selenium compounds, apoptosis and other types of cell death: an overview for cancer therapy. *Int. J. Mol. Sci.* **2012**, *13*, 9649–9672.
- (2) Fang, W. X.; Wu, P. W.; Hu, R. Z. Geochemical research of the impact of Se-Cu-Mo-V-bearing coal layers on the environment in Pingli County, Shaanxi Province, China. *J. Geochem. Explor.* **2003**, *80*, 105–115.
- (3) Schrauzer, G. N. Nutritional selenium supplements: product types, quality, and safety. *J. Am. Coll. Nutr.* **2001**, *20*, 1–4.
- (4) Margaret, P. R. The importance of selenium to human health. *Lancet* **2000**, *356*, 233–241.
- (5) Diaz-Alarcón, J. P.; Navarro-Alarcón, M.; López-García de la Serrana, H.; Asensio-Drima, C.; López-Martínez, M. C. Determination and chemical speciation of selenium in farmlands from southeastern Spain: relation to levels found in sugar cane. *J. Agric. Food Chem.* **1996**, *44*, 2423–2427.
- (6) Xu, J.; Zhu, S. G.; Yang, F. M.; Cheng, L. C.; Hu, Y.; Pan, G. X.; Hu, Q. H. The influence of selenium on the antioxidant activity of green tea. *J. Sci. Food Agric.* **2003**, *83*, 451–455.
- (7) Xu, J.; Yang, F. M.; Chen, L. C.; Hu, Q. H. Effect of selenium on increasing the antioxidant activity of tea leaves harvested during the early spring tea producing season. *J. Agric. Food Chem.* **2003**, *51*, 1081–1084.
- (8) Molan, A. L.; Flanagan, J.; Wei, W.; Moughan, P. J. Selenium-containing green tea has higher antioxidant and prebiotic activities than regular green tea. *Food Chem.* **2009**, *114*, 829–835.

- (9) Yu, F.; Sheng, J. C.; Xu, J.; An, X. X.; Hu, Q. H. Antioxidant activities of crude tea polyphenols, polysaccharides and proteins of selenium-enriched tea and regular green tea. *Eur. Food Res. Technol.* **2007**, *225*, 843–848.
- (10) Li, H. J.; Li, F.; Yang, F. M.; Fang, Y.; Xin, Z. H.; Zhao, L. Y.; Hu, Q. H. Size effect of Se-enriched green tea particles on *in vitro* antioxidant and antitumor activities. *J. Agric. Food Chem.* **2008**, *56*, 4529–4533.
- (11) Cabrera, C.; Artacho, R.; Giménez, R. Beneficial effects of green tea – a review. *J. Am. Coll. Nutr.* **2006**, *25*, 79–99.
- (12) Chen, H. X.; Zhang, M.; Qu, Z. S.; Xie, B. J. Antioxidant activities of different fractions of polysaccharide conjugates from green tea (*Camellia sinensis*). *Food Chem.* **2008**, *106*, 559–563.
- (13) Zhou, X. L.; Wang, D. F.; Sun, P. N.; Bucheli, P.; Li, L.; Hou, Y. F.; Wang, J. F. Effects of soluble tea polysaccharides on hyperglycemia in alloxan-diabetic mice. *J. Agric. Food Chem.* **2007**, *55*, 5523–5528.
- (14) Monobe, M.; Ema, K.; Kato, F.; Maeda-Yamamoto, M. Immunostimulating activity of a crude polysaccharide derived from green tea (*Camellia sinensis*) extract. *J. Agric. Food Chem.* **2008**, *56*, 1423–1427.
- (15) Dubois, M.; Gilles, K. A.; Hamilton, J. K.; Rebers, P. A.; Smith, F. Colorimetric method for determination of sugars and related substances. *Anal. Chem.* **1956**, *28*, 350–356.
- (16) Bitter, T.; Muir, H. M. A modified uronic acid carbazole reaction. *Anal. Biochem.* **1962**, *4*, 330–334.
- (17) Bradford, M. M. A rapid and sensitive method for the quantitation of microgram quantities of protein utilizing the principle of protein–dye binding. *Anal. Biochem.* **1976**, *72*, 248–254.
- (18) Lv, Y.; Yang, X.; Ruan, Y.; Yang, Y.; Wang, Z. Separation and quantification of component monosaccharides of the tea polysaccharides from *Gynostemma pentaphyllum* by HPLC with indirect UV detection. *Food Chem.* **2009**, *112*, 742–746.
- (19) Shang, D. J.; Zhang, J. N.; Wen, L.; Li, Y.; Cui, Q. Preparation, characterization, and antiproliferative activities of the Se-containing polysaccharide SeGLP-2B-1 from Se-enriched *Ganoderma lucidum*. *J. Agric. Food Chem.* **2009**, *57*, 7737–7742.
- (20) Li, W. J.; Nie, S. P.; Chen, Y.; Wang, Y. X.; Li, C.; Xie, M. Y. Enhancement of cyclophosphamide-induced antitumor effect by a novel polysaccharide from *Ganoderma atrum* in sarcoma 180-bearing mice. *J. Agric. Food Chem.* **2011**, *59*, 3707–3716.
- (21) He, N.; Yang, X.; Jiao, Y.; Tian, L.; Zhao, Y. Characterisation of antioxidant and antiproliferative acidic polysaccharides from Chinese wolfberry fruits. *Food Chem.* **2012**, *133*, 978–989.
- (22) Hsu, Y. L.; Chen, C. Y.; Hou, M. F.; Tsai, E. M.; Jong, Y. J.; Hung, C. H.; Kuo, P. L. 6-Dehydrogingerdione, an active constituent of dietary ginger, induces cell cycle arrest and apoptosis through reactive oxygen species/c-Jun N-terminal kinase pathways in human breast cancer cells. *Mol. Nutr. Food Res.* **2010**, *54*, 1307–1317.
- (23) Hsu, J. D.; Kao, S. H.; Ou, T. T.; Chen, Y. J.; Li, Y. J.; Wang, C. J. Gallic acid induces G2/M phase arrest of breast cancer cell MCF-7 through stabilization of p27<sup>kip1</sup> attributed to disruption of p27<sup>kip1</sup>/skp2 complex. *J. Agric. Food Chem.* **2011**, *59*, 1996–2003.
- (24) Huang, W. W.; Chiu, Y. J.; Fan, M. J.; Lu, H. F.; Yeh, H. F.; Li, K. H.; Chen, P. Y.; Chung, J. G.; Yang, J. S. Kaempferol induced apoptosis via endoplasmic reticulum stress and mitochondria-dependent pathway in human osteosarcoma U-2 OS cells. *Mol. Nutr. Food Res.* **2010**, *54*, 1585–1595.
- (25) Chou, C. C.; Yang, J. S.; Lu, H. F.; Ip, S. W.; Lo, C.; Wu, C. C.; Lin, J. P.; Tang, N. Y.; Chung, J. G.; Chou, M. J.; Teng, Y. H.; Chen, D. R. Quercetin-mediated cell cycle arrest and apoptosis involving activation of a caspase cascade through the mitochondrial pathway in human breast cancer MCF-7 cells. *Arch. Pharm. Res.* **2010**, *33*, 1181–1191.
- (26) Son, Y. O.; Hitron, J. A.; Wang, X.; Chang, Q. S.; Pan, J. J.; Zhang, Z.; Liu, J. K.; Wang, S. X.; Lee, J. C.; Shi, X. L. Cr(VI) induces mitochondrial-mediated and caspase-dependent apoptosis through reactive oxygen species-mediated p53 activation in JB6 Cl41 cells. *Toxicol. Appl. Pharmacol.* **2010**, *245*, 226–235.
- (27) Juan, M. E.; Wenzel, U.; Daniel, H.; Planas, J. M. Resveratrol induces apoptosis through ROS-dependent mitochondria pathway in HT-29 human colorectal carcinoma cells. *J. Agric. Food Chem.* **2008**, *56*, 4813–4818.
- (28) Li, L.; Lu, N.; Dai, Q.; Wei, L.; Zhao, Q.; Li, Z.; He, Q.; Dai, Y.; Guo, Q. GL-V9, a newly synthetic flavonoid derivative, induces mitochondrial-mediated apoptosis and G2/M cell cycle arrest in human hepatocellular carcinoma HepG2 cells. *Eur. J. Pharmacol.* **2011**, *670*, 13–21.
- (29) Zhang, H.; Zhang, M.; Yu, L.; Zhao, Y.; He, N.; Yang, X. B. Antitumor activities of quercetin and quercetin-5',8-disulfonate in human colon and breast cancer cell lines. *Food Chem. Toxicol.* **2012**, *50*, 1589–1599.
- (30) Van-Delft, M. F.; Huang, D. C. How the Bcl-2 family of proteins interact to regulate apoptosis. *Cell Res.* **2006**, *16*, 203–213.
- (31) Giono, L. E.; Manfredi, J. J. Mdm2 is required for inhibition of CDK2 activity by p21, thereby contributing to p53-dependent cell cycle arrest. *Mol. Cell. Biol.* **2007**, *27*, 4166–4178.
- (32) Satyanarayana, A.; Kaldis, P. A dual role of Cdk2 in DNA damage response. *Cell Div.* **2009**, *4*, 9–12.
- (33) Zhang, Y.; Luo, M.; Zu, Y.; Fu, Y.; Gu, C.; Wang, W.; Yao, L.; Efferth, T. Dryofragin, a phloroglucinol derivative, induces apoptosis in human breast cancer MCF-7 cells through ROS-mediated mitochondrial pathway. *Chem.–Biol. Interact.* **2012**, *199*, 129–136.
- (34) Nangia-Makker, P.; Conklin, J.; Hogan, V.; Raz, A. Carbohydrate-binding proteins in cancer, and their ligands as therapeutic agents. *Trends Mol. Med.* **2002**, *8*, 187–192.
- (35) Siegel, R.; Naishadham, D.; Jemal, A. Cancer statistics, 2012. *CA: Cancer J. Clin.* **2012**, *62*, 10–29.
- (36) Phil-Evans, W. Breast cancer screening: successes and challenges. *CA: Cancer J. Clin.* **2012**, *62*, 5–9.
- (37) Mitchell, D. B.; Santone, K. S.; Acosta, D. Evaluation of cytotoxicity in cultured cells by enzyme leakage. *Methods Cell Sci.* **1980**, *6*, 113–116.
- (38) Hafeez, B. B.; Siddiqui, I. A.; Asim, M.; Malik, A.; Afaq, F.; Adhami, V. M.; Saleem, M.; Din, M.; Mukhtar, H. A dietary anthocyanidin delphinidin induces apoptosis of human prostate cancer PC3 cells *in vitro* and *in vivo*: involvement of nuclear factor- $\kappa$ B signaling. *Cancer Res.* **2008**, *68*, 8564–8572.
- (39) Chipuk, J. E.; Kuwana, T.; Bouchier-Hayes, L.; Droin, N. M.; Newmeyer, D. D.; Schuler, M.; Green, D. R. Direct activation of Bax by p53 mediates mitochondrial membrane permeabilization and apoptosis. *Science* **2004**, *303*, 1010–1014.
- (40) El-Deiry, W. S.; Harper, J. W.; O'Connor, P. M.; Velculescu, V. E.; Canman, C. E.; Jackman, J.; Pietenpol, J. A.; Burrell, M.; Hill, D. E.; Wang, Y.; Wiman, K. G.; Mercer, W. E.; Kastan, M. B.; Kohn, K. W.; Elledge, S. J.; Kinzler, K. W.; Vogelstein, B. *WAF1/CIP1* is induced in p53-mediated G1 arrest and apoptosis. *Cancer Res.* **1994**, *54*, 1169–1174.
- (41) Thornberry, N. A.; Lazebnik, Y. Caspases: enemies within. *Science* **1998**, *281*, 1312–1316.
- (42) Vaculova, A.; Zhivotovsky, B. Caspases: determination of their activities in apoptotic cells. *Methods Enzymol.* **2008**, *442*, 157–181.
- (43) Sreelatha, S.; Jeyachitra, A.; Padma, P. R. Antiproliferation and induction of apoptosis by *Moringa oleifera* leaf extract on human cancer cells. *Food Chem. Toxicol.* **2011**, *49*, 1270–1275.
- (44) Gackowski, D.; Banaszkiwicz, Z.; Rozalski, R.; Jawien, A.; Olinski, R. Persistent oxidative stress in colorectal carcinoma patients. *Int. J. Cancer* **2002**, *101*, 395–397.
- (45) Lu, H. F.; Chen, Y. L.; Yang, J. S.; Yang, Y. Y.; Liu, J. Y.; Hsu, S. C.; Lai, K. C.; Chung, J. G. Antitumor activity of capsaicin on human colon cancer cells *in vitro* and Colo 205 tumor xenografts *in vivo*. *J. Agric. Food Chem.* **2010**, *58*, 12999–13005.